

Structural and magnetic properties of the complex perovskite oxide $\text{Ba}_2\text{HoHfO}_{5.5}$

J. Albino Aguiar, D. A. Landinez Tellez, Y. P. Yadava, and J. M. Ferreira
Departamento de Física, Universidade Federal de Pernambuco, 50670-901 Recife, PE, Brazil
 (Received 22 September 1997)

The complex cubic perovskite oxide $\text{Ba}_2\text{HoHfO}_{5.5}$ in the Ho-Ba-Hf-O rare-earth based oxide system has been prepared by a solid-state reaction process. Powder x-ray-diffraction studies show that $\text{Ba}_2\text{HoHfO}_{5.5}$ has an $A_2BB'O_6$ complex cubic perovskite structure. The x-ray-diffraction spectrum of single-phase $\text{Ba}_2\text{HoHfO}_{5.5}$ consists of strong peaks characteristics of a primitive cubic ABO_3 perovskite plus a few weak reflection lines arising from the superlattice. The presence of significant intensities of superstructure reflections in the x-ray spectrum of $\text{Ba}_2\text{HoHfO}_{5.5}$ acts as a signature for an ordered complex cubic perovskite oxide. Based on the doubling of primitive ABO_3 cubic perovskite unit cells, the lattice parameter of $\text{Ba}_2\text{HoHfO}_{5.5}$ calculated from the experimental x-ray diffraction is $a=8.316 \text{ \AA}$. The real part of the ac magnetic susceptibility of $\text{Ba}_2\text{HoHfO}_{5.5}$, measured in the temperature range 5 to 300 K shows a Curie-Weiss behavior. Using a Curie-Weiss law fitting we obtain an effective magnetic moment per Ho^{3+} ion in $\text{Ba}_2\text{HoHfO}_{5.5}$ of $9.33\mu_B$. This value is approximately 10% less than the spin-only moment ($10.60\mu_B$) expected for an isolated Ho ion. [S0163-1829(98)01029-7]

I. INTRODUCTION

Because of their varied structure and composition, perovskite materials have attracted intense research interest in many applied and fundamental areas of solid-state science and advanced materials research. Earlier works in 1950, and the 1960's¹⁻³ identified a large group of materials which have basic perovskite structure or a small distortion of that structure. These complex perovskite oxides generally have the formula $A_2BB'O_6$ or $A_3B_2B'O_9$ and result from the ordering of B and B' cations on the octahedral sites of the basic perovskite unit cell. Due to the increased complexity of the unit cell, a large variety of such materials are possible and hence a more continuous progression of lattice parameters can be produced. In recent years, complex perovskite oxides have been investigated as possible substrate materials for films of high- T_c superconductors,⁴⁻⁹ which are based on perovskite structure. The increased flexibility in the lattice parameter constant of complex cubic perovskite oxides enable a better match of the substrate lattice parameter to that of the high- T_c superconductor film. In view of these considerations, in the course of our research program on the development of new substrates for high- T_c superconductors, we have synthesized a rare-earth complex perovskite oxide $\text{Ba}_2\text{HoHfO}_{5.5}$, in the rare-earth-based Ho-Ba-Hf-O oxide system using a solid-state synthesis process. As detailed structural knowledge such as crystal structure and superstructural ordering phenomenon in such complex cubic perovskite oxides is important for understanding the electronic behavior as well as to evaluate their potential candidature as a substrate material for high- T_c superconductor films, we have carried out a structural study of $\text{Ba}_2\text{HoHfO}_{5.5}$ using powder x-ray diffraction (XRD). We, have also studied magnetic properties of this material by measuring the ac magnetic susceptibility in the temperature range 5–300 K.

II. EXPERIMENTAL DETAILS

Holmium barium hafnate $\text{Ba}_2\text{HoHfO}_{5.5}$ in the Ho-Ba-Hf-O system was synthesized using a solid-state reaction

process. Stoichiometric ratio of high purity constituent chemicals (purity 99.99%) Ho_2O_3 , BaCO_3 , and HfO_2 were thoroughly mixed in an agate mortar and the mixed powder was dried for 6 h at a temperature of 200 °C. Dried powder was compacted as a circular disc (diameter of 10 mm and thickness of 1–2 mm) and calcined at a temperature of 1100 °C for 40 h in ambient atmosphere. The calcined material was cooled down slowly to room temperature and again finely powdered using an agate mortar. Finally, ground calcined powder was compacted at a pressure of 5 ton/cm² in the form of a circular disc and sintered at 1200 °C for various durations of time (40–60 h) in ambient atmosphere. The sintered materials were slowly cooled down to room temperature. At all stages of the calcination and sintering the processed material was examined by powder x-ray diffraction (XRD). The XRD spectra were recorded at room temperature by a Siemens D-5000 x-ray diffractometer using Cu $K\alpha$ radiation ($\lambda=1.5406 \text{ \AA}$). Magnetic properties of the $\text{Ba}_2\text{HoHfO}_{5.5}$ were investigated in the temperature range 5–300 K by measuring the ac magnetic susceptibility in zero dc

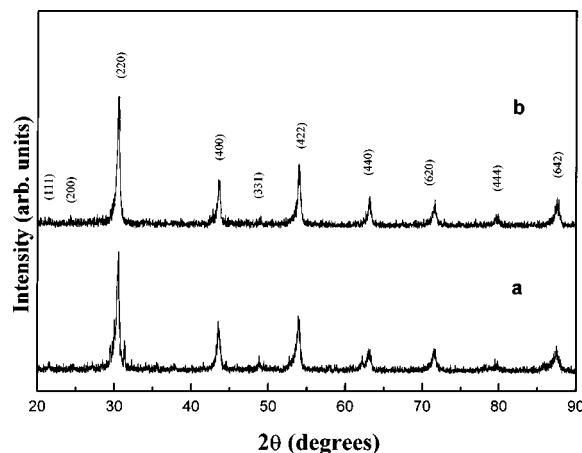


FIG. 1. X-ray spectrum of $\text{Ba}_2\text{HoHfO}_{5.5}$, (a) sintered at 1200 °C for 40 h and (b) sintered at 1200 °C for 60 h.

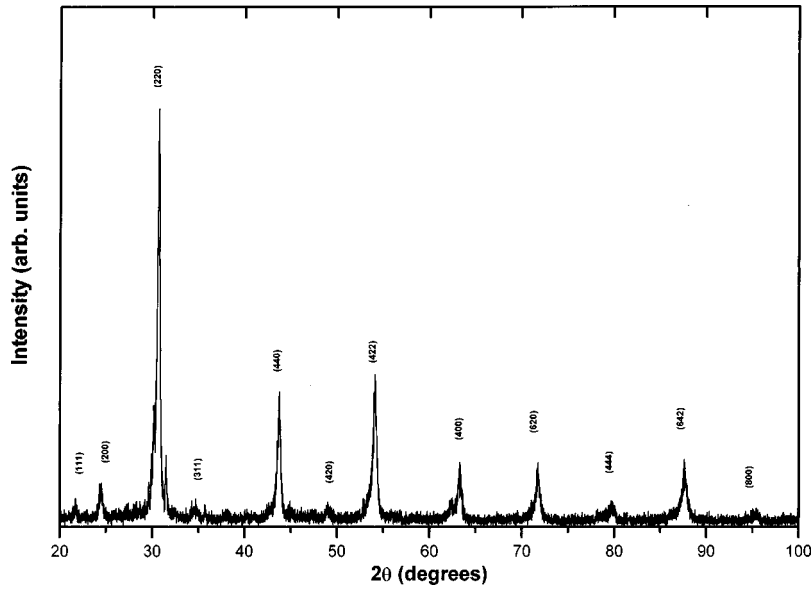


FIG. 2. X-ray-diffraction spectra of single-phase $\text{Ba}_2\text{HoHfO}_{5.5}$ with $t=2.5$ sec and step = 0.01.

applied magnetic field, at a frequency of 31 Hz and with an ac field amplitude of 3 Oe, using a Quantum Design (MPMS-5S) superconducting quantum interference device (SQUID) magnetometer.

III. RESULTS AND DISCUSSION

A powder x-ray-diffraction spectrum of $\text{Ba}_2\text{HoHfO}_{5.5}$ sintered at 1200°C for 40 h and 1200°C for 60 h are shown in Figs. 1(a) and 1(b), respectively. The XRD spectra of $\text{Ba}_2\text{HoHfO}_{5.5}$ sintered at 1200°C for 40 h shows a predominant cubic perovskite phase and we were able to obtain single-phase $\text{Ba}_2\text{HoHfO}_{5.5}$ with complex cubic perovskite structure only by sintering at 1200°C for 60 h. The XRD spectra of single-phase $\text{Ba}_2\text{HoHfO}_{5.5}$ for 2θ between 5 and 100 degrees, taken at a slow scanning time of 2.5 sec is shown in Fig. 2. It consists of strong peaks which are characteristics of a primitive cubic perovskite plus a few weak line reflections arising from the superlattice. No evidence for a distortion from the cubic symmetry is observed in the XRD spectrum. The basic perovskite composition is ABO_3 , where A is a large ion suitable to the 12-coordinated cube-octahedral sites and B is a smaller ion suitable to the 6-coordinated octahedral site. Complex perovskite with mixed species on a site (particularly the B site) may be represented by multiples of this formula unit and a larger unit cell, e.g., $A_2BB'O_6$, $A_3B_2B'O_9$, etc.⁷ Thus in the $\text{Ba}_2\text{HoHfO}_{5.5}$ composition, Ba^{2+} with the largest ionic radius (1.34 Å) occupies position A , Ho^{3+} (ionic radius 0.894 Å) and Hf^{4+} (ionic radius 0.78 Å) cations occupy the B and B' positions in the B site due to their smaller ionic radii compared to that of the Ba^{2+} cation. Due to the ordering of B and B' on the octahedral site of the ABO_3 unit cell there is a doubling in the lattice parameter of the basic cubic perovskite unit cell. Thus, the whole XRD pattern of $\text{Ba}_2\text{HoHfO}_{5.5}$ can be indexed in a $A_2BB'O_6$ cubic cell with the cell edge $a=2a_p$ where a_p is the cell lattice of the cubic perovskite. The XRD spectrum of $\text{Ba}_2\text{HoHfO}_{5.5}$ is similar to $A_2BB'O_6$ -type complex cubic perovskite oxides, e.g., YBa_2NbO_6 , $\text{ErBa}_2\text{SbO}_6$, $\text{DyBa}_2\text{NbO}_6$, etc., reported in the JCPDS file, as judged by the similarity in d spacings and intensity ratios.

The presence of the superstructure reflection lines (111) and (311) in the XRD spectrum of $\text{Ba}_2\text{HoHfO}_{5.5}$ is the signature of an ordered complex cubic perovskite structure. In a substitutional solid solution BB' , there is a random arrangement of B and B' on equivalent lattice positions in the crystal structure. It upon suitable heat treatment, the random solid solution rearranges into a structure in which B and B' occupy the same set of positions but in a regular way, such a structure is described as superstructure. In the superstructure, the positions occupied by B and B' are no longer equivalent and this feature is exhibited in the XRD spectrum of the material by the presence of superstructure reflection lines.¹⁰

For a double cubic perovskite of the formula $A_2BB'O_6$ the intensity, in particular of the (111) superstructure reflection, is proportional to the difference in scattering power of the B and B' atoms, when all the atoms are situated in the ideal position.¹¹ A disordered arrangement of B and B' should result in zero intensity. Therefore Ho^{3+} and Hf^{4+} cation ordering in $\text{Ba}_2\text{HoHfO}_{5.5}$ in B and B' positions is clearly distinguished by the presence of the significant intensity of (111) and (311) superstructural reflection lines.

Based on above discussion we have now indexed the XRD peaks of $\text{Ba}_2\text{HoHfO}_{5.5}$ as an ordered complex cubic

TABLE I. X-ray-diffraction data of $\text{Ba}_2\text{HoHfO}_{5.5}$.

2θ	d (Å)	I/I_0	hkl
21.702	4.0916	6.42	111
24.420	3.6421	9.73	200
30.648	2.9147	100.00	220
34.231	2.6174	4.55	311
43.701	2.0696	31.26	400
48.981	1.8581	6.00	420
54.078	1.6944	30.64	422
63.259	1.4688	11.18	440
71.715	1.3150	15.32	620
79.693	1.2022	4.76	444
87.511	1.1138	13.87	642
95.078	1.0441	4.10	800

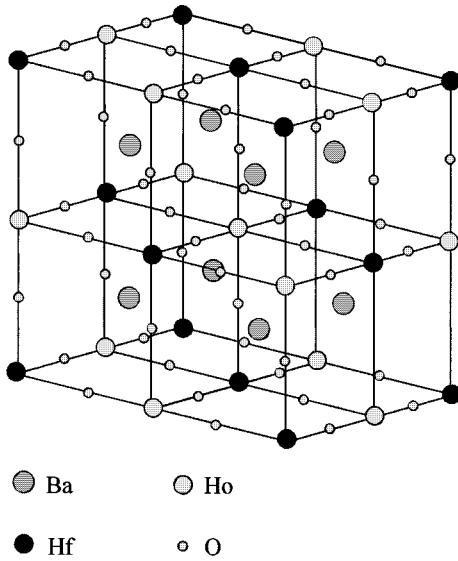


FIG. 3. Crystal structure diagram of $\text{Ba}_2\text{HoHfO}_{5.5}$.

perovskite with $A_2BB'O_6$ crystal structure. XRD data of $\text{Ba}_2\text{HoHfO}_{5.5}$ obtained from the XRD spectrum are tabulated in Table I. The lattice parameter of $\text{Ba}_2\text{HoHfO}_{5.5}$, calculated from the experimental XRD data is $a_{\text{exp}} = 8.316 \text{ \AA}$.

For $A_2BB'O_6$ materials, based on the ionic radii as given in Shannon and Prewitt¹² and using a hard sphere approximation, an average value of the lattice parameter a_{cal} can be calculated theoretically, using the relations

$$a_A = 2(R_A + R_O) \times (2^{-1/2}), \quad (1)$$

$$a_B = R_B + R_{B'} + 2R_O, \quad (2)$$

and

$$a_{\text{cal}} = (a_A + a_B) / 2, \quad (3)$$

where R_A , R_B , $R_{B'}$, and R_O are the ionic radii of A, B, B' cations, respectively, and anion oxygen. a_A and a_B are the calculated lattice parameter, based on A and B cations, a_{cal} is the average calculated lattice parameter. Using relations (1)–(3), we obtained an average value of 8.075 \AA for the lattice

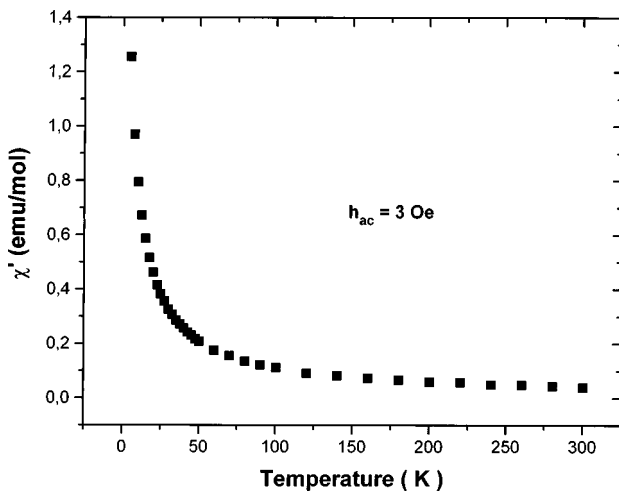


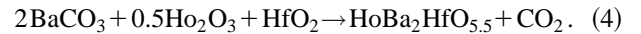
FIG. 4. Real part of the ac magnetic susceptibility versus temperature curve for $\text{Ba}_2\text{HoHfO}_{5.5}$.

TABLE II. Curie-Weiss parameters for Ho^{3+} in $\text{Ba}_2\text{HoHfO}_{5.5}$, determined from the magnetic ac susceptibility measurements.

C (emu K/mol)	θ_p (K)	χ_0 (emu/mol)	$\mu_{\text{eff}} (\mu_B)$
10.848	-3.781	7.38×10^{-3}	9.33

constant a_{cal} of $\text{Ba}_2\text{HoHfO}_{5.5}$, which is 2.98% smaller than the experimental value $a_{\text{exp}} = 8.316 \text{ \AA}$. Similar differences have been observed in experimental and theoretical values of lattice parameter in some other $A_2BB'O_6$ type perovskite oxides such as YBa_2NbO_6 and $\text{DyBa}_2\text{SbO}_6$. Taking into account the doubling of the basic perovskite unit cell, the complex cubic perovskite crystalline structure of $\text{Ba}_2\text{HoHfO}_{5.5}$ is represented in Fig. 3.

Though $\text{Ba}_2\text{HoHfO}_{5.5}$ has $A_2BB'O_6$ structure, taking into account the valence of 4^+ for Hf, the chemical formula of this compound is written as $\text{Ba}_2\text{HoHfO}_{5.5}$ according to the chemical reaction



In Fig. 4 we show the temperature dependence of the real part of the ac magnetic susceptibility for $\text{Ba}_2\text{HoHfO}_{5.5}$ measured in zero dc applied magnetic field, at a frequency of 31 Hz and with an ac field amplitude of 3 Oe. The magnetic susceptibility of $\text{Ba}_2\text{HoHfO}_{5.5}$ agrees well with the Curie Weiss law

$$\chi = \chi_0 + C / (T - \theta_p), \quad (5)$$

where C is the Curie constant [$C = N(\mu_{\text{eff}})^2 / 3k_B$], N is Avogadro's number, μ_{eff} is the effective magnetic moment ($\mu_{\text{eff}} = p_{\text{eff}} \mu_B$), p_{eff} is the effective Bohr magneton (μ_B) number, k_B is the Boltzmann constant, θ_p is the paramagnetic Curie temperature, and χ_0 is the temperature-independent susceptibility term.

The magnetic parameters for Ho^{3+} in $\text{Ba}_2\text{HoHfO}_{5.5}$, estimated from the Curie-Weiss law [Eq. (5)] are given in Table II. The value of the constant susceptibility term χ_0 is

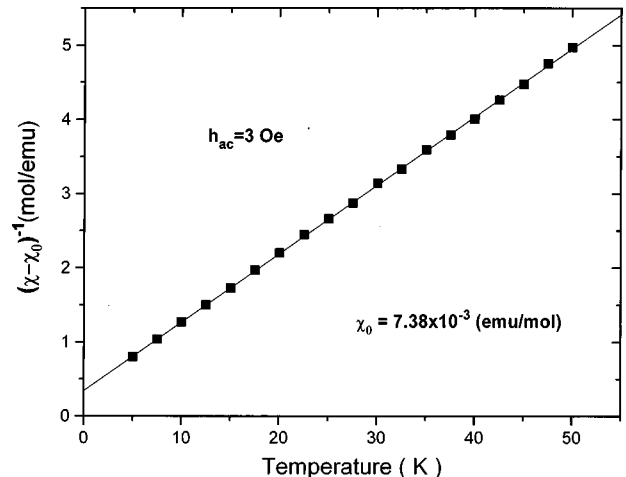


FIG. 5. $(\chi - \chi_0)^{-1}$ versus temperature curve for $\text{Ba}_2\text{HoHfO}_{5.5}$ with $\chi_0 = 7.38 \times 10^{-3} \text{ emu/mol}$. The solid curve shows a fitted Curie-Weiss line.

7.38×10^{-3} emu/mol which may arise from the Van Vleck paramagnetic contribution.

Figure 5 shows the reciprocal of the real part of the ac magnetic susceptibility $(\chi - \chi_0)^{-1}$ as a function of temperature with $(\chi_0 = 7.38 \times 10^{-3}$ emu/mol). The Curie Constant C , estimated from the solid line in Fig. 5 is $C = 10.848$ emu K/mol, and the effective magnetic moment per Holmium ion calculated from this constant is $9.33 \mu_B$ which is approximately 10% less than the spin-only moment ($10.60 \mu_B$) expected for an isolated Ho^{3+} ion. One possible explanation for the discrepancy between the observed and theoretical values is the crystal field effects which screen the effective moment of the magnetic ion.

IV. CONCLUSIONS

In conclusion, we have synthesized a complex perovskite oxide $\text{Ba}_2\text{HoHfO}_{5.5}$ in the rare-earth-based Ho-Ba-Hf-O ox-

ide system. X-ray diffraction studies show that it has a complex cubic perovskite structure. Significant presence of superstructure reflections (111) and (311) in the XRD spectrum of $\text{Ba}_2\text{HoHfO}_{5.5}$ reveal that it is an ordered $A_2B_2B'O_6$ complex cubic perovskite material with lattice constant $a = 8.316$ Å, calculated from the experimental x-ray-diffraction data. ac magnetic susceptibility of $\text{Ba}_2\text{HoHfO}_{5.5}$, measured in the temperature range 5–300 K, exhibits a Curie-Weiss behavior. The effective magnetic moment of Ho^{3+} ion in $\text{Ba}_2\text{HoHfO}_{5.5}$ $9.33 \mu_B$ is approximately 10% less than the spin-only moment ($10.60 \mu_B$) expected for an isolated Ho^{3+} ion.

ACKNOWLEDGMENTS

This work was financed by Brazilian Research Agencies CNPq and FINEP. D.A.L.T. acknowledges CNPq and the Colombian Science Agencies, Colciencias.

¹R. Roy, *J. Am. Ceram. Soc.* **37**, 581 (1954).

²F. Galasso, L. Katz, and R. Ward, *J. Am. Ceram. Soc.* **81**, 820 (1959).

³F. Galasso, J. R. Borrante, and L. Katz, *J. Am. Ceram. Soc.* **83**, 2830 (1961).

⁴C. D. Brandle and V. J. Fratello, *J. Mater. Res.* **5**, 2160 (1990).

⁵J. Koshy, K. S. Kumar, J. Kurian, Y. P. Yadava, and A. D. Damoderan, *J. Am. Ceram. Soc.* **78**, 3088 (1995).

⁶I. T. Kim, Y. H. Kim, and S. J. Chung, *Jpn. J. Appl. Phys., Part 1* **34**, 4096 (1995).

⁷V. J. Fratello, C. W. Berkstresser, C. D. Brandle, and A. J. Van

Graitis, *J. Cryst. Growth* **166**, 878 (1996).

⁸J. Koshy, J. Kurian, K. S. Kumar, P. K. Sajith, M. J. Asha, and R. Jose, *Indian J. Pure Appl. Phys.* **34**, 698 (1996).

⁹R. Jose, A. M. John, J. Kurian, P. K. Sajith, and J. Koshy, *J. Mater. Res.* **12**, 2976 (1997).

¹⁰A. F. Wells, *Structural Inorganic Chemistry*, 5th ed. (Clarendon, Oxford, 1986), p. 279.

¹¹W. T. Fu and D. J. Ijdo, *J. Solid State Chem.* **128**, 323 (1997).

¹²R. D. Shannon and C. T. Prewitt, *Acta Crystallogr., Sect. B: Struct. Crystallogr. Cryst. Chem.* **25**, 925 (1969).